ELectronics EXpress

LETTER

IEICE Electronics Express, Vol.14, No.10, 1–6

A microstrip-fed *W*-band waveguide filter using H-shaped coupling slots

Yu Xiao, Tang Li, and Houjun Sun[a)]

Beijing Key Laboratory of Millimeter Wave and Terahertz Technology, School of Information and Electronics, Beijing Institute of Technology, Beijing, 100081, China

a) *sunhoujun@bit.edu.cn*

Abstract: A novel microstrip-fed waveguide filter is proposed in this letter. The H-shaped slots on the back side of the substrate are utilized to connect waveguide cavities and the microstrip circuit. Simultaneously, they are used to realize external coupling of the filter. This design can effectively reduce the size of the circuit and avoid extra transition loss, which is good for system integration. A fifth-order filter at *W*-band based on H-shaped coupling slots have been fabricated and measured. Good agreements between the simulated and measured results are observed.

Keywords: H-shaped coupling slot, *W*-band, filter, waveguide

Classification: Microwave and millimeter-wave devices, circuits, and modules

References

[1] C. Riva, *et al.*: "The challenge of using the *W*-band in satellite communication," Int. J. Satell. Commun. Netw. **32** (2014) 187 (DOI: 10.1002/sat.1050).

[2] L. Yujiri, *et al.*: "Passive millimeter wave imaging," IEEE Microw. Mag. **4** (2003) 39 (DOI: 10.1109/MMW.2003.1237476).

[3] Z. C. Hao, *et al.*: "Developing low-cost, *W*-band SIW bandpass filters using the commercially available printed-circuit-board technology," IEEE Trans. Microw. Theory Techn. **64** (2016) 1775 (DOI: 10.1109/TMTT.2016.2553029).

[4] C. A. Leal-Sevillano, *et al.*: "A pseudo-elliptical response filter at *W*-band fabricated with thick SU-8 photo-resist technology," IEEE Microw. Wireless Compon. Lett. **22** (2012) 105 (DOI: 10.1109/LMWC.2012.2183861).

[5] S. Song, *et al.*: "*W*-Band bandpass filter using micromachined air-cavity resonator with current probes," IEEE Microw. Wireless Compon. Lett. **20** (2010) 205 (DOI: 10.1109/LMWC.2010.2042552).

[6] J. S. Hong and M. J. Lancaster: *Microstrip Filters for RF/Microwave Applications* (Wily, New York, 2001).

[7] R. J. Cameron: "Advanced coupling matrix synthesis techniques for microwave filters," IEEE Trans. Microw. Theory Techn. **51** (2003) 1 (DOI: 10.1109/TMTT.2002.806937).

[8] Z. Yang, *et al.*: "A rectangular waveguide filter with integrated E-plane probe transition," IEICE Electron. Express **14** (2017) 20161108 (DOI: 10.1587/elex.13.20161108).

[9] V. Rathi, *et al.*: "Improved coupling for aperture coupled microstrip antennas," IEEE Trans. Antennas Propag. **44** (1996) 1196 (DOI: 10.1109/8.511831).

DOI: 10.1587/elex.14.20170326
Received April 1, 2017
Accepted April 10, 2017
Publicized April 21, 2017
Copyedited May 25, 2017

[10] J.-H. Lee, *et al.*: "A V-band front-end with 3-D integrated cavity filters/duplexers and antenna in LTCC technologies," IEEE Trans. Microw. Theory Techn. **54** (2006) 2925 (DOI: 10.1109/TMTT.2006.877440).
[11] J. W. Bandler, *et al.*: "Space mapping: the state of the art," IEEE Trans. Microw. Theory Techn. **52** (2004) 337 (DOI: 10.1109/TMTT.2003.820904).
[12] X. Shang, *et al.*: "*W*-Band waveguide filters fabricated by laser micromachining and 3-D printing," IEEE Trans. Microw. Theory Techn. **64** (2016) 2572 (DOI: 10.1109/TMTT.2016.2574839).
[13] K. Li, *et al.*: "A *W* band low-loss waveguide-to-microstrip probe transition for millimeter-wave applications," Int. Microw. Millimeter Wave Circuits Syst. Technol. Workshop (2012) 1 (DOI: 10.1109/MMWCST.2012.6238136).

1 Introduction

The interest in radio astronomy and image radar applications at *W*-band (75–110 GHz) has increased recently [1, 2]. Filters with low insertion loss and high selectivity are key components of RF front-ends in these systems. In recent years, some emerging techniques have been reported to develop *W*-band filters. In [3], although the filter based substrate integrated waveguide (SIW) technology shows the advantage of easy integration, the minimum insertion loss is up to 3.21 dB in pass-band due to lack of quality factor and fabrication accuracy at *W*-band. The air-filled waveguide filters including using milling process and micro-machined technology have high quality factor and low insertion loss. However, integrating them into planar circuits is difficult, and the transition structures between waveguide filters and planar circuits are required. These transition structures cause space consuming and increase transmission loss. Besides, the micro-machined technology such as SU-8 photoresist technology [4], and deep reactive ion etching process [5] result in high fabrication cost.

In this letter, a low-cost waveguide filter using milling process with low insertion loss for easy integration at *W*-band is proposed. The input and output ports of the filter are microstrip feedlines rather than waveguides. The H-shaped slots are utilized to connect resonant waveguide cavities and the planar microstrip circuit. Moreover, they are used to realize external coupling of the filter, which is simply controlled by adjusting the sizes of H-shaped slots. Thus, this configuration can effectively avoid space consuming and extra transition loss.

2 Configuration and design

The proposed filter is shown in Fig. 1, which consists of three parts. The bottom part is the waveguide resonant cavities. The middle part is Rogers RT/Duroid 5880 substrate with relative permittivity of 2.2 and height of 127 um. And, the top part is the shield cover. Two input/output microstrip feedlines with 50 ohm port impedance are etched on the top side of the substrate. Two H-shaped slots etched on the back side of the substrate are used to couple the energy from input/output microstrip feedlines into the first and last cavity resonators, respectively. It's noted that, some metallized vias with 0.4 mm diameter on the substrate are deliberately designed to ensure a good grounding contact between the bottom cavities and

DOI: 10.1587/elex.14.20170326
Received April 1, 2017
Accepted April 10, 2017
Publicized April 21, 2017
Copyedited May 25, 2017

the shield cover and decrease the electromagnetic interference at such a high-frequency band.

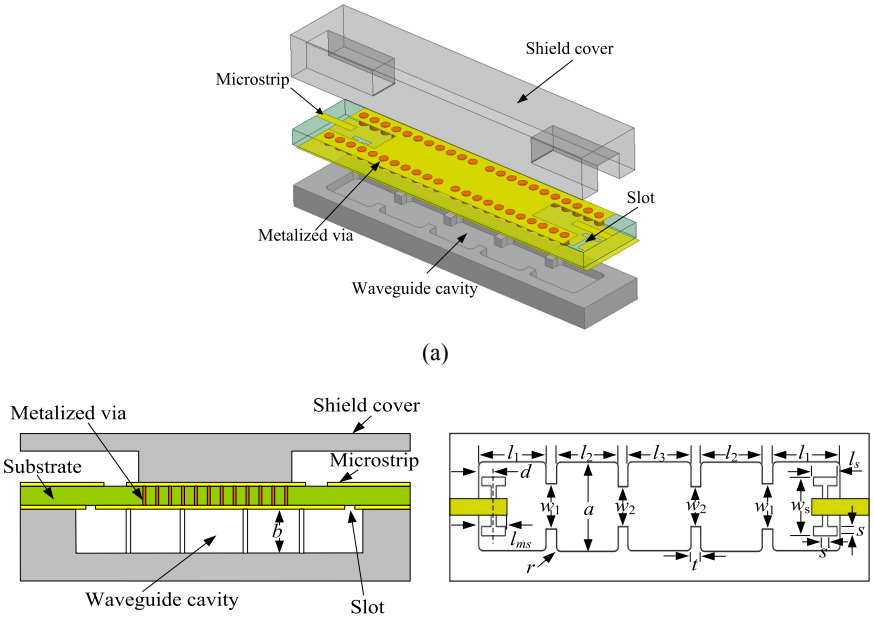

Fig. 1. Configuration of the proposed rectangular waveguide filter: (a) 3D exploded view (b) sectional view (c) top view

In this letter, the bandpass filter developed works at the center frequency (f_0) of 92.75 GHz with the bandwidth (BW) of 2.5 GHz. The filter is synthesized with the theory of coupled resonator circuits [6]. According to this theory, the performance of the filter is mainly determined by the resonant frequency f_i of the ith resonator (R_i), the coupling coefficient k_{ij} between the R_i and R_j, and the external quality factor Q_e ($i, j = 1, 2, 3, 4, 5$ and $i \neq j$). Using the method in [7], the generalized coupling matrix of low-pass circuit prototype can be written as

$$M = \begin{bmatrix} & S & 1 & 2 & 3 & 4 & 5 & L \\ S & 0 & 1.014 & 0 & 0 & 0 & 0 & 0 \\ 1 & 1.014 & 0 & 0.865 & 0 & 0 & 0 & 0 \\ 2 & 0 & 0.865 & 0 & 0.636 & 0 & 0 & 0 \\ 3 & 0 & 0 & 0.636 & 0 & 0.636 & 0 & 0 \\ 4 & 0 & 0 & 0 & 0.636 & 0 & 0.865 & 0 \\ 5 & 0 & 0 & 0 & 0 & 0.865 & 0 & 1.014 \\ L & 0 & 0 & 0 & 0 & 0 & 1.014 & 0 \end{bmatrix} \quad (1)$$

The design parameters (f_i, k_{ij} and Q_e) can be then calculated by de-normalizing the generalized element values of the generalized coupling matrix as follows

$$k_{ij} = FBW \cdot M_{ij}, \quad Q_e = \frac{1}{FBW \cdot M_{S1}^2}, \quad FBW = \frac{BW}{f_0} \quad (2)$$

where FBW is the relative bandwidth. In this case, $k_{12} = k_{45} = 0.023$, $k_{23} = k_{34} = 0.017$, and $Q_e = 36.1$. Besides, all the resonators are synchronously tuned at $f_1 = f_2 = f_3 = f_4 = f_5 = f_0 = 92.75$ GHz.

DOI: 10.1587/elex.14.20170326
Received April 1, 2017
Accepted April 10, 2017
Publicized April 21, 2017
Copyedited May 25, 2017

On the other hand, the design parameters are related to physical dimensions of the filter. Like traditional iris metal waveguide filter, the cross-section size of the resonant cavity is selected to support only the dominant TE_{10} mode propagation. The longitudinal length of each resonant cavity is about $\lambda_g/2$ to excite the TE_{101} resonant mode. As in Fig. 2(a), the coupling coefficient k_{ij} can be extracted from EM simulation results of the coupled resonators using the following equation [6]

$$k_{ij} = \frac{f_{p2}^2 - f_{p1}^2}{f_{p2}^2 + f_{p1}^2} \tag{3}$$

where f_{p1} and f_{p2} represent the lower and upper resonator frequency of the coupled resonators, respectively.

In most occasions, external coupling of the waveguide filter is realized with an iris. In [8], the E-plane microstrip probe is introduced into the design of an *X*-band waveguide filter to implement the external coupling, which is good for decreasing the circuit size. However, in this structure, the microstrip probes are perpendicular to waveguide cavities so that the filter is difficult to integrate with the planar microstrip circuit. In our filter, the H-shaped slot is employed to realize the external coupling as in Fig. 1(c). In contrast to the rectangular slot of the same length, the H-shaped slot gives more coupling, which can achieve wider Q_e range [9]. To maximize coupling, the optimum length of the microstrip stub (l_{ms}) is about $\lambda_g/5$ [10]. The H-shaped slot is initially positioned at $l_1/4$ from the edge of the cavity. Generally, w_s is chosen to be approximately $\lambda_g/4$, and l_s is $\lambda_g/8$. Fig. 2(b) shows the relationship between the width of the slot (s) and the Q_e extracted from the EM simulation using [6]

$$Q_e = \frac{f_0}{\Delta f_{\pm 90^\circ}} \tag{4}$$

where f_0 is the resonant frequency of input/output resonator, and the value of $\Delta f_{\pm 90^\circ}$ is the absolute bandwidth between the phase shifts of ±90° points with respect to the absolute phase at f_0.

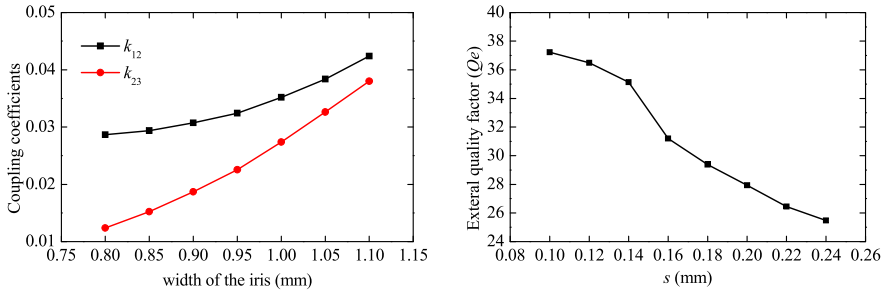

(a) (b)

Fig. 2. (a) The coupling coefficients between different resonators (b) The extracted external quality factor Q_e versus the width of the slot

Once all initial physical dimensions are obtained by using the curves in Fig. 2, optimization process will be carried on to satisfy the desired specifications. In order to speed up the optimization process, the well-known aggressive space mapping (ASM) optimization algorithm is used [11]. To this end, two models named as the coarse and fine model need to be established at first. The fine model, as in Fig. 1, is

DOI: 10.1587/elex.14.20170326
Received April 1, 2017
Accepted April 10, 2017
Publicized April 21, 2017
Copyedited May 25, 2017

established in the full-wave simulator HFSS. The coarse model is designed by the fast equivalent circuit model solver ADS as shown in Fig. 3, where the lumped RLC elements represent the resonators and the quarter-wavelength transmission lines with electrical length 90° are used to represent the couplings. *Z*ref is the characteristic impedance of the transmission line. The actual physical parameter X_f includes six geometrical variables in the fine mode, while the corresponding variables derived from the coupling matrix consist of the parameter X_c in the coarse model. They are expressed as

$$\begin{aligned} X_f &= [l_1 \quad l_2 \quad l_3 \quad w_1 \quad w_2 \quad s] \\ X_c &= [f_1 \quad f_2 \quad f_3 \quad k_{12} \quad k_{23} \quad Q_e] \end{aligned} \tag{5}$$

These circuit parameters in Fig. 3 can be related to X_c by the following equations [6]

$$\begin{aligned} Ci &= \frac{Q_e}{2\pi f_i Z} \times 10^{12} \quad Li = \frac{Z}{2\pi f_i Q_e} \times 10^9 \\ Z01 &= Z \quad Zij = \frac{Z}{Q_e k_{ij}} \end{aligned} \tag{6}$$

where $Z = 50$ ohm is the terminal impedance at the input/output ports, and the unit of f_i is Hz. After a few of iterations using ASM optimization algorithm, the simulation result of the fine model in HFSS meet the requirements of the specification. Table I gives the optimized values of physical dimensions.

Table I. Key physical dimensions of the filter (units: millimeters)

a	b	l_1	l_2	l_3	w_1	w_2
2	0.4	2.53	2.35	2.38	1.01	0.92
t	r	d	l_{ms}	l_s	w_s	s
0.4	0.2	0.56	0.81	0.63	1.03	0.2

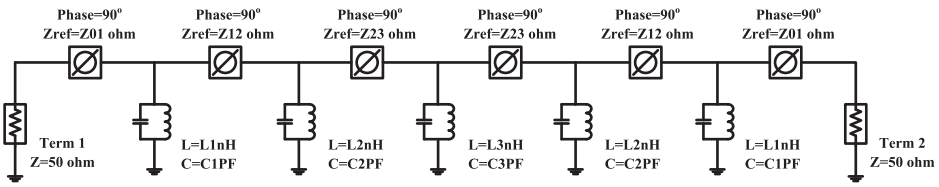

Fig. 3. The coarse model in ADS

3 Simulation and experiment results

The metal surface roughness at *W*-band can't be ignored, which yields a reduced effective conductivity. In the simulation, the effective conductivities of waveguide cavities are set as 7.04×10^6 S/m [12]. The solid curve in Fig. 5 shows that the simulated minimum in-band insertion loss is 1.75 dB. In order to measure the filter with standard WR10 test interface, two classical microstrip-to-waveguide transitions in [13] are adopted. The filter cascading two transitions has been fabricated as shown in Fig. 4. The measurement is carried out by Agilent VNA with FEV-10-TR frequency extension module. The measured in-band minimum insertion loss of the filter with two transitions as shown by dash curve in Fig. 5 is 3.2 dB. Considering

DOI: 10.1587/elex.14.20170326
Received April 1, 2017
Accepted April 10, 2017
Publicized April 21, 2017
Copyedited May 25, 2017

the measured typical insertion loss of the back-to-back transition is about 1 dB [13], the in-band insertion loss of the filter should be better than 2.2 dB. The measured insertion loss is about 0.45 dB worse than the simulated one. This could be caused by the assembly error between waveguide cavities and the substrate.

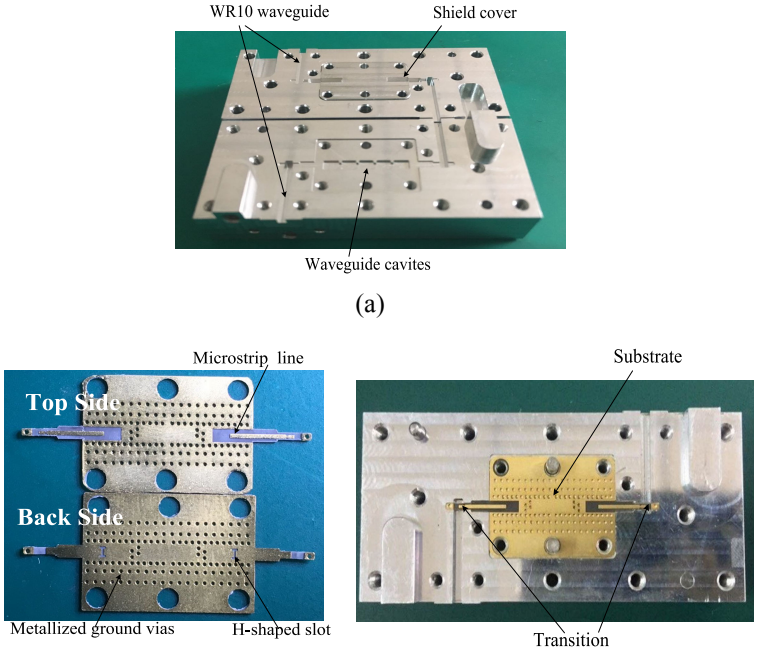

Fig. 4. Photograph of the fabricated filter: (a) The waveguide cavities and the shield cover of the filter (b) The etched pattern on each side of the substrate (c) The assembly relationship between the substrate and the waveguide cavities

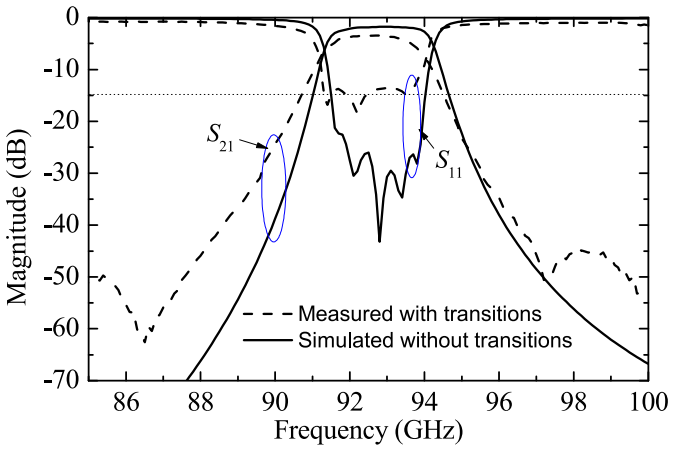

Fig. 5. The frequency responses of the filter

4 Conclusion

A novel fifth-order waveguide filter at *W*-band with microstrip feedlines is presented in this letter. By introducing the H-shaped slots on the back side of the substrate, the filter can effectively reduce the size of the circuit and avoid extra transition loss. The measured results agree with the simulated ones. The proposed filter will be a good candidate for *W*-band millimeter wave front-ends applications.

DOI: 10.1587/elex.14.20170326
Received April 1, 2017
Accepted April 10, 2017
Publicized April 21, 2017
Copyedited May 25, 2017